ELSEVIER

Journal of Photochemistry and Photobiology A: Chemistry 95 (1996) 103-110

Journal of PHOTOCHEMISTRY AND PHOTOBIOLOGY A:CHEMISTRY

Kinetic studies of ground-state atomic caesium, $Cs(6\,^2S_{1/2})$, by time-resolved laser-induced fluorescence ($Cs(7\,^2P_{3/2}$–$6\,^2S_{1/2})$; $\lambda = 455.5$ nm) following pulsed irradiation

E. Martinez [a],*, J. Albaladejo [a], A. Notario [a], D. Husain [b]

[a] *Departamento de Quimica Fisica, Facultad de Ciencias Quimicas, Universidad de Castilla - La Mancha, 13071 - Cuidad Real, Spain*

[b] *Department of Chemistry, University of Cambridge, Lensfield Road, Cambridge CB2 1EW, UK*

Received 26 June 1995; accepted 13 October 1995

Abstract

We present a kinetic investigation of atomic caesium in its electronic ground state at elevated temperature by laser-induced fluorescence (LIF). A detailed description is given of a new apparatus in which $Cs(6\,^2S_{1/2})$ is generated in a stainless steel reactor from the broad-band pulsed irradiation of CsCl vapour at an elevated temperature and monitored by LIF using the shorter-wavelength component of the Rydberg doublet via the transition at $\lambda = 455.5$ nm ($Cs(7\,^2P_{3/2}$–$6\,^2S_{1/2})$) using boxcar integration and computerized analysis. LIF decay profiles for $Cs(6\,^2S_{1/2})$ in excess helium alone at various temperatures indicate diffusional loss. Decay profiles were also investigated at different total pressures with mixtures of an added reactant R of fixed relative composition $f = [R]/([R]+[He])$ with excess He buffer gas from which absolute rate data were extracted, essentially for single elevated temperatures for various added gases. The following absolute second-order rate constants k_R are reported for the removal of $Cs(6\,^2S_{1/2})$ by different reactants: N_2O, $(1.1 \pm 0.4) \times 10^{-10}$ cm^3 molecule^{-1} s^{-1} ($T = 723$–753 K); CH_3Cl, $(5.4 \pm 0.2) \times 10^{-12}$ cm^3 molecule^{-1} s^{-1} (830 K); CF_3Cl, $(3.0 \pm 0.2) \times 10^{-11}$ cm^3 molecule^{-1} s^{-1} (830 K); CF_2Cl_2, $(1.5 \pm 0.5) \times 10^{-11}$ cm^3 molecule^{-1} s^{-1} (830 K); $CFCl_3$, $(1.2 \pm 0.1) \times 10^{-10}$ cm^3 molecule^{-1} s^{-1} (830 K); C_2H_5Cl, $(1.5 \pm 0.5) \times 10^{-11}$ cm^3 molecule^{-1} s^{-1} (830 K). Whilst the collisional behaviour of $Cs(6\,^2S_{1/2})$ has been investigated by direct monitoring in the time domain using various methods, we believe the present investigation to constitute the first study of these processes in the presence of the chloride reactants by LIF. With the exception of $CFCl_3$, where the lower value of the reaction rate constant obtained by atomic resonance absorption spectroscopy is attributed to thermal decomposition in the static reactor, there is reasonable agreement between the two techniques. Although the present result for $k_R(Cs + N_2O)$ using LIF is significantly larger than that obtained by resonance absorption, it is in accord with previous measurements using LIF, supporting the present method for characterising kinetic data for $Cs(6\,^2S_{1/2})$ at elevated temperatures.

Keywords: Atomic caesium; Ground state; Kinetic studies; Pulse irradiation; Laser-induced fluorescence

1. Introduction

Whilst there have been a range of experimental investigations on alkali atoms in the time domain in recent years leading to absolute rate data for reaction [1–3], kinetic measurements on the heaviest of the alkali atoms, $Cs(6\,^2S_{1/2})$, have only been the object of limited study by time-resolved methods. The collisional behaviour of this atom is particularly important on account of its low first ionization potential (3.893 90 eV [4]), a fundamental property critical to any collisional mechanism involving electron transfer. The investigation of rate processes undergone by Cs in flames have been reported, including diffusion [5] and third-order recombination involving $Cs + O_2 + M$ [6,7], and one is bound also to note that the reaction between $Cs + CCl_4$ was seminal in the development of molecular beam investigations of alkali atom collisions [8]. A significant body of absolute rate data on $Cs(6\,^2S_{1/2})$ has been obtained from measurements in the time domain resulting from atomic resonance absorption spectroscopy following pulsed irradiation including data for reactions with molecular halogens [9–12], N_2O [13], third-order recombination with O_2 [14] and halogen atom abstraction from alkyl halides and similar reactants [15,16]. From the viewpoint of monitoring in the time domain, third-order reactions involving $Cs + OH + He$ and $Cs + I + He$ employed time-resolved molecular resonance fluorescence and atomic resonance fluorescence on OH [17] and I [18] respectively in the presence of excess Cs and He. Previous kinetic investigations on caesium involving lasers have principally been concerned with the production of $Cs(6\,^2S_{1/2})$ by laser pho-

---

* Corresponding author.

SSDI 1010-6030(95)04253-9

tolysis of CsI vapour and subsequent monitoring of the Cs atom using a second laser by resonance ionization spectroscopy [19–21]. Plane [3] has reported detailed kinetic data for the reaction of Cs + N_2O by LIF following pulsed irradiation. In this paper we describe the construction of a versatile apparatus for the generation of Cs(6 $^2S_{1/2}$) by broad-band pulsed photolysis of a caesium halide with subsequent time-resolved monitoring of the atom at the Rydberg transition at $\lambda = 455.5$ nm (Cs(7 $^2P_{1/2}$–6 $^2S_{1/2}$)) by laser-induced fluorescence (LIF). The diffusion of Cs(6 $^2S_{1/2}$) in the helium bath gas is described, and the absolute rates are presented for reaction with N_2O, a standard for atomic kinetic investigation, and for reactants with a range of chlorine-containing molecules. The resulting data are compared, where appropriate, with absolute rate data for the study of Cs + N_2O reported by Plane [3] but mainly with data derived from time-resolved atomic resonance absorption spectroscopy.

2. Experimental details

Kinetic studies of lithium, sodium and potassium atoms by time-resolved LIF investigations have been established in recent years, particularly by Plane and coworkers [22–24]. Reactions of Cs with N_2O and with various chloride molecules are investigated here by the time-resolved LIF study of Cs atoms employing the shorter-wavelength component of the strong spin–orbit-resolved Rydberg doublet transition at $\lambda = 455.5$ nm (Cs(7 $^2P_{1/2,3/2}$)–Cs(6 $^2S_{1/2}$); $\lambda = 459.318$ and 455.536 nm; $gA = 0.65 \times 10^8$ and 1.4×10^8 s^{-1} respectively [25,26]); in preference to the longer-wavelength D-line emission (6 $^2P_{1/2,3/2}$–6 $^2S_{1/2}$; $\lambda = 894.350$ and 852.110 nm; $gA = 0.48 \times 10^8$ and 1.3×10^8 s^{-1} respectively [25,26]) on account of the sensitivity of the photomultiplier tube employed (Thorn EMI 9813 B, Bialk.) and the pumping efficiency of laser dyes at these longer wavelengths.

The experiments were performed using a newly constructed apparatus that is shown schematically in Fig. 1. The reactor is entirely constructed from stainless steel to facilitate working at high temperatures and to present a relatively inert surface to hot reagent gases. It comprises a central cylindrical chamber with a vertical arm ($r = 2.5$ cm; $l = 6.0$ cm) directly above this to provide optical coupling for measuring the LIF signal from the centre of the chamber below. Two orthogonal pairs of tubes enter the central chamber half-way along the vertical side of the cylinder. One pair of opposite arms (tube radius, 1.1 cm) provides an optical coupling for the flash-lamp which is used to photolyse CsCl vapour at an elevated temperature in the central chamber. A pair of opposite arms provides an optical axis for the probe laser, with windows set at the Brewster angle and baffles inserted inside to exclude scattered light from the central chamber. All arms were sealed with quartz windows and Viton O-rings. The parts placed behind the windows are cooled by water that circulates into copper tubes around the arms to prevent vapour from condensing on the windows. The reactor is enclosed in a furnace made in a new light material (Newtherm 1000; density, 260 kg m^{-3}) which contains four resistances (Kanthal-1) that can heat both the vessel and about half the length of the side arm to over 1200 K. The temperature inside the reactor is monitored with a chrome–alumel thermocouple (Ni–Cr–Ni, type K) placed in a small stainless steel tube welded to the wall of the central chamber near the reaction zone. Once the selected temperature has been reached, the temperature controller (Jumo dTRON 16) maintains this temperature of the gas inside the reactor to within ±5 °C.

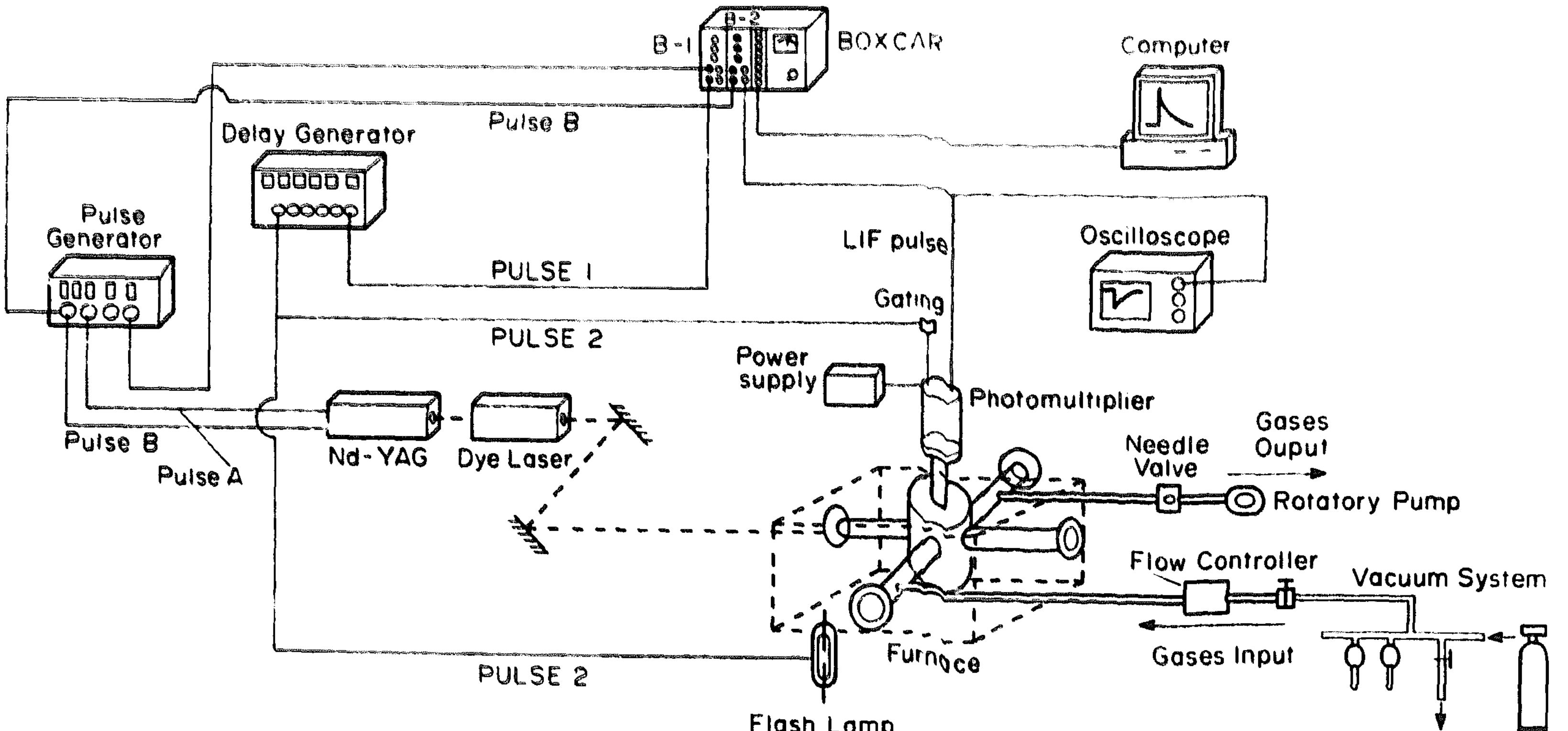

Fig. 1. Block diagram of the experimental arrangement for the kinetic study of atomic caesium, Cs(6 $^2S_{1/2}$), generated by pulsed irradiation at an elevated temperature and monitored by time-resolved LIF at $\lambda = 455.5$ nm (Cs(7 $^2P_{3/2}$–6 $^2S_{1/2}$)).

A mixture of known relative concentration of the reagent gas (N_2O or an alkyl chloride) in He is made in an all-glass vacuum system and slowly flowed through the reactor. The flow rate of this mixture is selected with a flow controller (ASM model LB1B) placed at the exit of the reactor. The total pressure in this zone is measured with a calibrated capacitance manometer (Leybold CM100 rank 10^{-2}–10^2 Torr). Typically, the total mass flow was 50 standard $cm^3\ min^{-1}$ except for the reaction with N_2O when this was 200 standard $cm^3\ min^{-1}$. The evacuation of both the gas line, storage bulbs and reactor prior to preparation of gaseous reagents was achieved by the combined used of a rotary vacuum pump (Telstar model RD-18; 18 $m^3\ h^{-1}$) and a home-made oil diffusion pump with liquid-nitrogen traps. Pressures as low as about $(4–5)\times10^{-5}$ Torr were routinely achieved. The quality of the vacuum was measured with a 10^{-4}–10^3 Torr Pirani gauge (Leybold model TR 901).

$Cs(6\ ^2S_{1/2})$ was generated in the central chamber by pulsed irradiation of CsCl vapour at elevated temperature [27]. The CsCl precursor was employed as the photochemical source of the caesium atom [28] in order to minimize the effects of halogen atom exchange between the precursor source and the reactant mixture (in the case of the reactions with alkyl chlorides) on admission to the high temperature reaction vessel. Kinetic measurements on $Cs(6\ ^2S_{1/2})$ were made on time scales by which the electronically excited atoms, $Cs(6\ ^2P_J)$ [29] and $Cl(3\ ^2P_{1/2})$ [30], generated in the photolysis, had been fully relaxed. The photolysis source was an externally triggered high pressure Xe flash-lamp system (JML-SP10; maximum pulse energy, 8 J at 10 Hz) specially designed to meet the requirements of the present system. (We are particularly indebted to Dr. Gert Rapp of the University of Heidelberg, Germany, for considerable assistance in the design of this pulsed lamp system.) This system consists of two units: the power supply and the flash-lamp housing which also contains the optical elements to focus loosely the beam (2 cm in diameter) into the middle of the central chamber, and the 10 μF fast-discharge storage capacitor to minimize the electromagnetic noise generated by the system. The flash-lamp is characterized, according to the manufacturer, by a black-body temperature of 12 000 K and the half-width of the light pulse is about 15 μs.

The probe laser for inducing fluorescence from caesium atoms is a pulsed dye laser (Continuum ND60) pumped by a neodymium-doped yttrium aluminium garnet (Nd:YAG) laser (Continuum NY 81CS-10) which provides pulses of 6 ns with 0.08 cm^{-1} bandwidth resolution. The dye that was used is Coumarin 460 (Exciton) and the dye-laser was employed at energies of less than 1 mJ per pulse to avoid any saturation effects. LIF signals were monitored by a gated photomultiplier tube (Thorn EMI 9813 B; gating circuit Thorn EMI GB1A) attached to the vertical arm of the reactor after passing through an interference filter centred at $\lambda = 455.5$ nm (CWL; FWB, 2 nm). The voltage at which the photomultiplier tube was operated varied between 1.5 and 1.9 kV depending on the size of the LIF pulse. The output from the photomultiplier tube is terminated in a 10 kΩ resistor in order to increase the apparent lifetime of the LIF pulse to the microsecond scale. The signal is then input into the gated integrator of a boxcar averager (Stanford Research Systems model SR 250) and finally transferred to a computer via an SR245 computer interface (Stanford Research Systems model SR245) for subsequent analysis.

The entire experiment is controlled by a pulse delay generator (Stanford Research Systems model DG 535) (pulses 1 and 2 in Fig. 2) in combination with a double-pulse generator (Pulsetek model 233) used to fire externally the probe laser, and another SR250 boxcar averager unit (B1) used to scan the probe laser with respect to the photolysis flash. Two TTL pulses (about 100 μs wide) are needed in order to fire the Nd:YAG laser externally: pulse A to trigger the flash-lamps, and pulse B to trigger the *Q*-switch electronics. The optimum delay between these two pulses for maximum output power is about 550 μs.

Fig. 2 illustrates the repetitive sequence of pulses for two different reactions times corresponding to two different delays (delays 1 and 2) between the photolysis flash and the probe laser output. An initial TTL pulse (pulse 1) is sent from the delay generator (DG 535) to the boxcar unit (B1) whose gate is scanned using the data acquisition program (SR 270, Stanford Research Systems) and used to trigger the Pulsetek pulse generator that fires the probe laser. A second pulse from the DG 535 unit (pulse 2) is used to trigger the

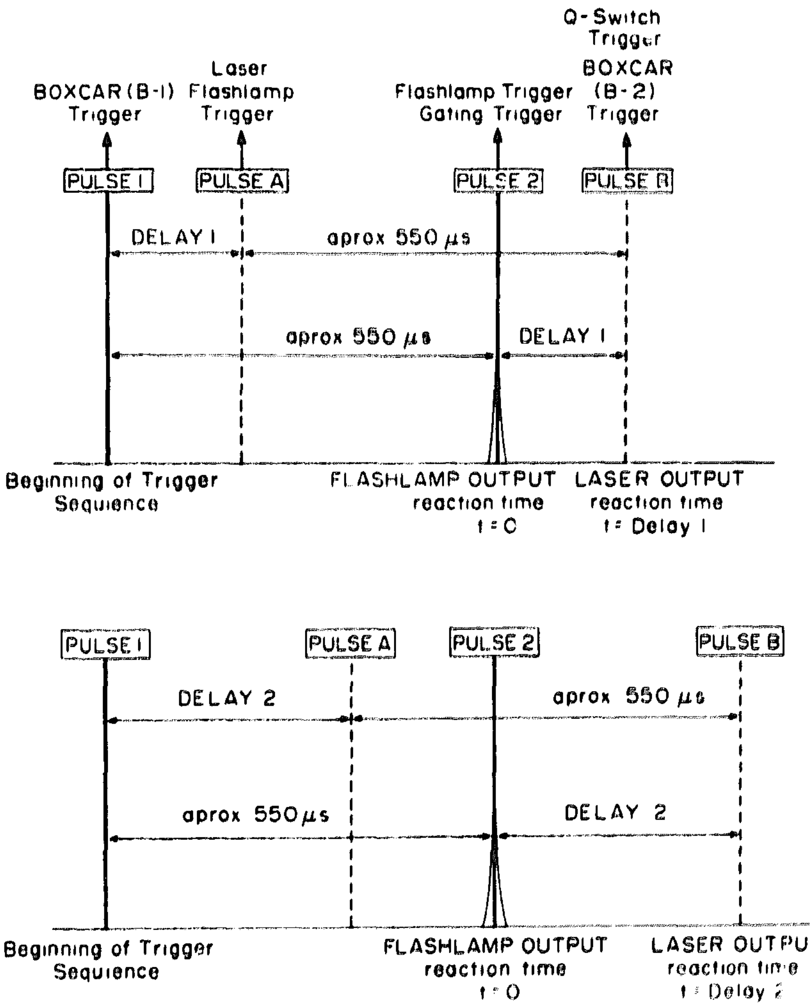

Fig. 2. Diagram of the timing sequences for the kinetic study of $Cs(6\ ^2S_{1/2})$, generated by pulsed irradiation at an elevated temperature, and monitored by time-resolved LIF at $\lambda = 455.5$ nm ($Cs(7\ ^2P_{3/2}–6\ ^2S_{1/2})$).

photomultiplier tube gating circuit and the photolysis flashlamp. The delay between pulses 1 and 2 is adjusted to the same value as the delay between pulses A and B. As a result, at a reaction time equal to zero (when the delay of boxcar B1 gate is zero), the output of the probe laser coincides with the photolysis flash, and scanning the boxcar B1 gate (delays 1, 2 etc.), we may consequently scan the laser with respect to the photolysis flash. Pulse B, which coincides with the laser output, may also be used to trigger boxcar B2 that integrates the LIF signal collected by the photomultiplier tube.

The photomultiplier gating circuit reduces the gain of the photomultiplier tube by a factor of 10^3 during the first 40 μs of the reaction to avoid amplification of the scattered light from the photolysis flash and any tailing effects are eliminated when setting an initial delay of 100 μs. Thus we neglect the first 100 μs of the reaction and the acquisition begins about 650 μs after the start of the firing sequence. The delay scanned by the integrated averager gate ranges from a few hundred microseconds to a few milliseconds, depending on the lifetime of the caesium atoms formed in the flash. Each scan was divided into 200 bins and normally averaged four times to improve the signal-to-noise ratio. The DG 535 unit typically triggered the firing sequence at a repetition rate of 5 Hz.

2.1. Materials

Helium (purity, 99.999%; Carburos Metálicos) was used without further purification. N_2O (purity, 99.99%; Carburos Metálicos) and the alkyl chlorides (CH_3Cl (purity, 99.5%; Argon S.A.); CF_3Cl (purity, 99.7%, Argon S.A.); CF_2Cl_2 (purity, 99.7%, Argon S.A.); C_2H_5Cl (purity, 99.7%, Argon S.A.) and CF_3Cl (purity, 99.9%, Carburos Metálicos)) were degassed at 77 K before use. CsCl (purity, 99.9%, Aldrich) was refluxed in the reaction at 700 K for several hours prior to kinetic measurements.

3. Results and discussion

3.1. Diffusion of Cs(6 $^2S_{1/2}$) in He

Fig. 3 gives examples of the digitized time variation of the laser-induced fluorescence I_F at $\lambda = 455.5$ nm (Cs(7 $^2P_{3/2}$)) → Cs(6 $^2S_{1/2}$) + $h\nu$) representing the decay of ground-state atomic caesium, generated from the pulsed irradiation of CsCl vapour at $T = 780$ K in the presence of various pressures of He. Such profiles are fitted by computer to the standard form

$$I_F = \Theta_1 + \Theta_2 \exp(-k't) \qquad (1)$$

where Θ_1 represents the long-time component of the scattered light and k' is the first-order decay coefficient of Cs(6 $^2S_{1/2}$) which is the object of kinetic interest in these investigations. In this instance, the first-order decay coefficient due to diffusional removal ($k' = \beta'$) would, of course, be expected to demonstrate an inverse proportionality with the total pressure ($\beta' = \beta/p_T$). Husain and Bing Ji [13] have previously described measurements on the diffusional decay of Cs(6 $^2S_{1/2}$) in He alone and have characterized the diffusion coefficient D_{12}(Cs–He) at elevated temperatures [13] assuming removal of Cs(6 $^2S_{1/2}$) at the walls of the reaction vessel on every collision using the "long-time solution" of the diffusion equation for a cylinder of defined length and radius [31,32]. In the present measurements, assignment of boundary conditions is difficult to define in terms of the geometry of the optical excitation and light collection processes. Further, given the very limited temperature variation that can be employed with the present experimental system (see Section 2), and the relatively small variation in diffusion coefficients with temperature in general, the temperature dependence of D_{12}(Cs–He) could not be determined accurately [13]. In the present measurements, we are primarily concerned with the dependence of the diffusional loss term on pressure rather than its detailed value. This can be seen in Fig. 4 which gives examples of the linear relationship between k' for diffusion vs. $1/p_{He}$ across a limited range of temperatures. This form is subsequently employed in the kinetic analysis for the reactions of Cs(6 $^2S_{1/2}$).

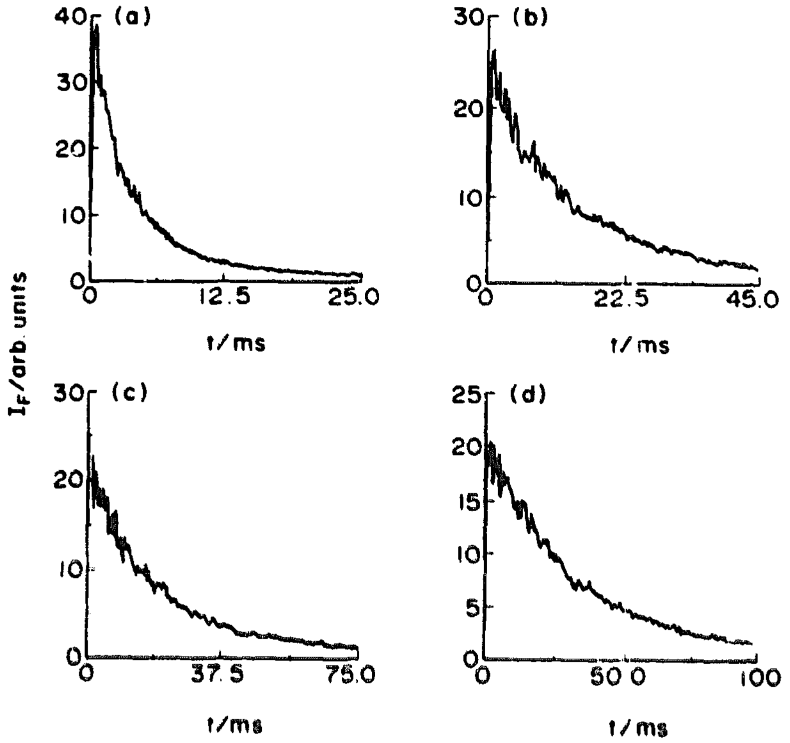

Fig. 3. Examples of the digitized time variation in the LIF at $\lambda = 455.5$ nm (Cs(7 $^2P_{3/2}$–6 $^2S_{1/2}$)), indicating the decay of atomic caesium by diffusion following the pulsed irradiation of CsCl vapour at an elevated temperature ($T = 780$ K) in the presence of different pressures p_{He} of helium buffer gas: (a) 7.9 Torr; (b) 39.2 Torr; (c) 47.9 Torr; (d) 82.3 Torr.

3.2. Reaction of Cs(6 $^2S_{1/2}$) + N_2O

The kinetic behaviour of a metal atom with the molecule N_2O constitutes a convenient kinetic test of the system especially in view of the inert reaction product N_2. As with previous resonance absorption measurements on Cs + N_2O [14], LIF decay profiles for Cs(6 $^2S_{1/2}$) were recorded for different total pressures p_T from a dilute mixture of N_2O + He of fixed relative composition f (= $[N_2O]/([He] + [N_2O])$). The overall first-order rate coefficient k' for the transient atom

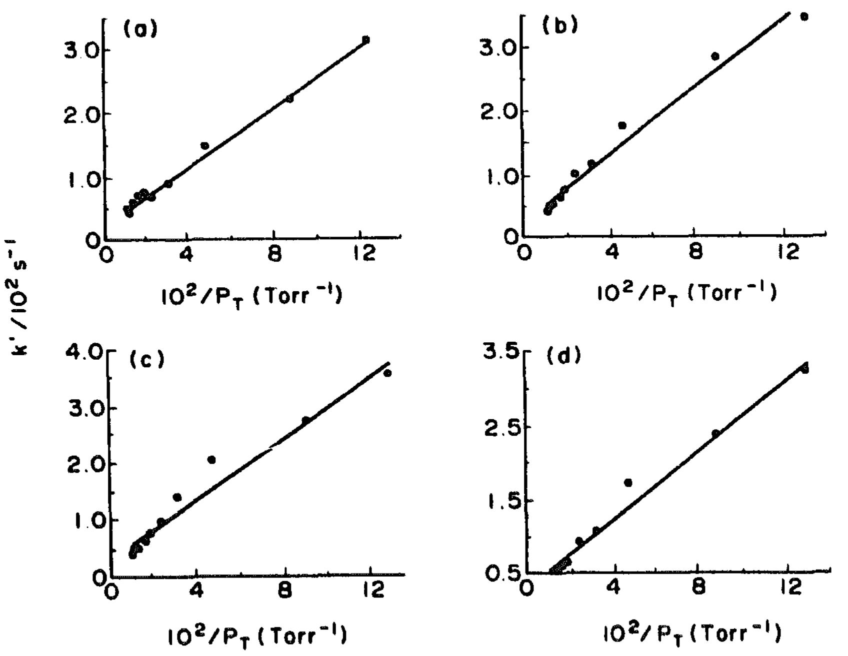

Fig. 4. Examples of the variation in the first-order decay coefficient k' for the decay of Cs(6 $^2S_{1/2}$) obtained by LIF at $\lambda = 455.5$ nm (Cs(7 $^2P_{3/2}$–6 $^2S_{1/2}$)) following the pulsed irradiation of CsCl vapour in the presence of different pressures p_T of helium buffer gas at different temperatures T: (a) 750 K; (b) 800 K; (c) 830 K; (d) 876 K.

was characterized in each case by computerized fitting to Eq. (1) of the LIF profiles of the type given in Fig. 5, which demonstrates examples of the decay of the caesium atom at different total pressures in an N_2O–He mixture at $T = 773$ K. This procedure thus involves the simultaneous variation in the decay of Cs(6 $^2S_{1/2}$) by the reaction

$$Cs + N_2O \longrightarrow CsO + N_2 \qquad (2)$$

together with loss by diffusion. A similar approach used for the kinetic study of reactions of Cs + RCl. This approach avoids the onerous task of preparing large numbers of dilute mixtures of N_2O or RCl and He at a constant total pressure in order to maintain a constancy in the relatively small diffusional loss with the variation in k' due to reaction (2) or its analogue with a chlorine-containing molecule.

Combining the kinetic effects of diffusional removal and chemical reaction of Cs(6 $^2S_{1/2}$) with N_2O (reaction (2)) in a series of measurements of the type indicated in Fig. 5, the variation in the overall first-order rate coefficient for the caesium atom may be expressed in the standard form

$$k' = \frac{\beta}{p_T} + k_2 f p_T \qquad (3)$$

where the absolute second-order rate constant for the reaction of Cs + N_2O (k_2) now involves the appropriate units of pressure. Equation (3) may be recast in the form

$$k' p_T = \beta + k_2 f p_T^2 \qquad (4)$$

and hence a plot of $k' p_T$ vs. p_T^2 yields k_2 using the appropriate values of f. Results are shown in Fig. 6 for the removal of Cs(6 $^2S_{1/2}$) with N_2O at various temperatures. The data are too scattered to yield reliable Arrhenius parameters at the elevated temperature range over which the reaction has been investigated which is too small to extract an activation energy. Similar behaviour was observed in the analogous study using time-resolved resonance absorption measurements where Husain and Bing Ji [13] report $k_2 = (1.9 \pm 0.3) \times 10^{-11}$ cm³ molecule⁻¹ s⁻¹ for the temperature range 847–865 K. In the present investigation, the absolute rate data are more scattered at elevated temperatures, presumably on account of effects of thermal decomposition of N_2O on the stainless steel so that

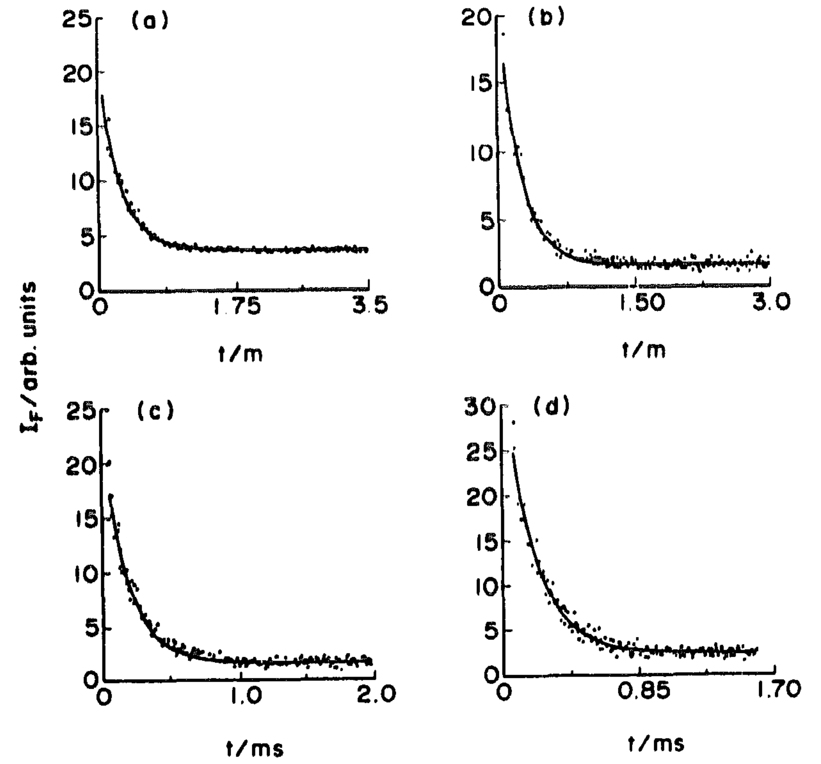

Fig. 5. Examples of the digitized time variation in the LIF at $\lambda = 455.5$ nm (Cs(7 $^2P_{3/2}$–6 $^2S_{1/2}$)) indicating the decay of atomic caesium in the presence of N_2O and helium buffer gas following the pulsed irradiation of CsCl vapour at an elevated temperature ($T = 773$ K; $f = [N_2O]/([He] + [N_2O]) = 6.4 \times 10^{-5}$): (a) $p_T = 15.3$ Torr; (b) $p_T = 31.1$ Torr; (c) $p_T = 41.0$ Torr; (d) $p_T = 70.2$ Torr.

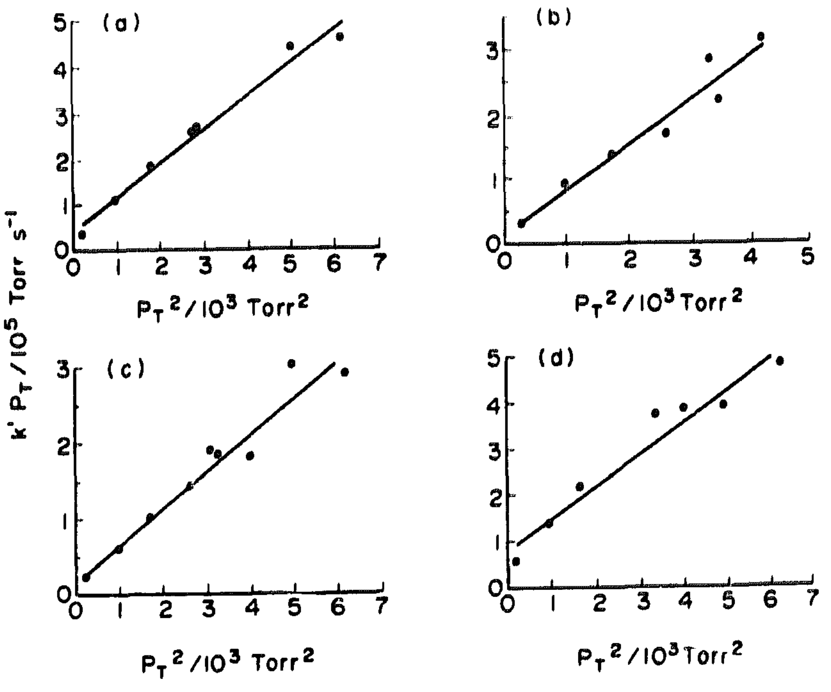

Fig. 6. Examples of the variation in the first-order decay coefficient k' for the decay of Cs(6 $^2S_{1/2}$) obtained by LIF at $\lambda = 455.5$ nm (Cs(7 $^2P_{3/2}$–6 $^2S_{1/2}$)) following the pulsed irradiation of CsCl vapour in the presence of different total pressures p_T of N_2O and helium buffer gas i.e. $k' p_T$ vs. p_T^2 at different temperatures ($f = [N_2O]/([He] + [N_2O])$): (a) $T = 723$ K, $f = 4.6 \times 10^{-5}$; (b) $T = 773$ K, $f = 5.0 \times 10^{-5}$; (c) $T = 737$ K, $f = 3.7 \times 10^{-5}$; (d) $T = 773$ K, $f = 6.4 \times 10^{-5}$.

kinetic data at lower temperatures are considered more reliable for which we report $k_2 = (1.1 \pm 0.4) \times 10^{-10}$ cm^3 molecule^{-1} s^{-1} (T = 723–753 K) where the range indicates the spread of values of k_2 rather than errors of plots of the type given in Fig. 6 and indicating a result significantly larger than reported by resonance absorption [13]. The result, however, is in agreement with that for k_2 studied by LIF as a function of temperature by Plane [3]. Rate constants calculated from that study yields k_2 (723 K) and k_2 (753 K) as $(1.42 \pm 0.03) \times 10^{-10}$ cm^3 molecule^{-1} s^{-1} and $(1.49 \pm 0.02) \times 10^{-10}$ cm^3 molecule^{-1} s^{-1} respectively. Thus the two studies of the reaction of Cs + N_2O by LIF are in accord within the errors quoted and indicate that the earlier value reported from time-resolved resonance absorption spectroscopy is too low, presumably on account of thermal and chemical decomposition of N_2O in the static reactor employed in that investigation [13].

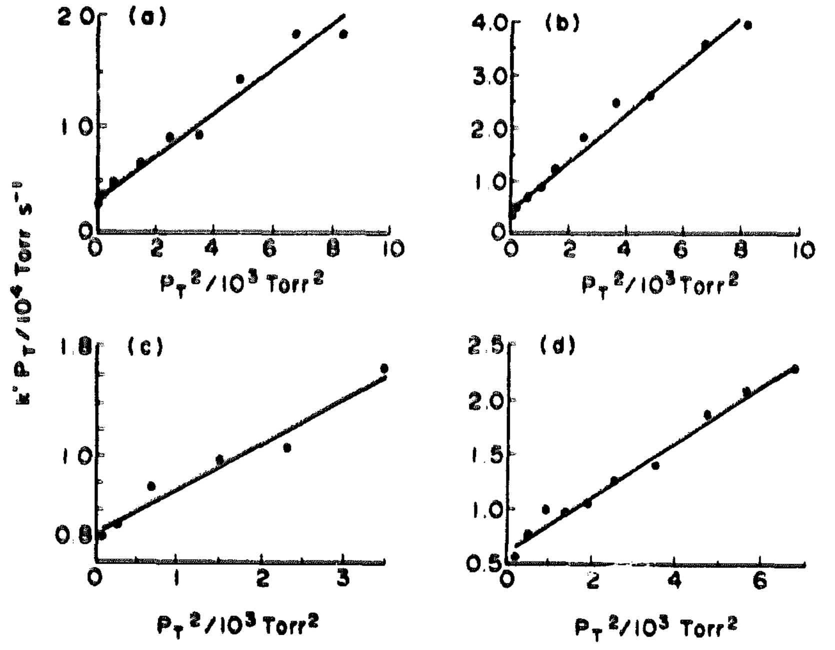

Fig. 7. Examples of the variation in the first-order decay coefficient k' for the decay of Cs(6 $^2S_{1/2}$) obtained by LIF at λ = 455.5 nm (Cs(7 $^2P_{3/2}$–6 $^2S_{1/2}$)) following the pulsed irradiation of CsCl vapour in the presence of different total pressures p_T of CH_3Cl and helium buffer gas i.e. $k'p_T$ vs. p_T^2 at different temperatures (f = [CH_3Cl]/([He] + [CH_3Cl])): (a) T = 780 K, $f = 5.3 \times 10^{-5}$; (b) T = 780 K, $f = 7.9 \times 10^{-5}$; (c) T = 800 K, $f = 5.3 \times 10^{-5}$; (d) T = 830 K, $f = 4.9 \times 10^{-5}$.

3.3. Reaction of Cs(6 $^2S_{1/2}$) + CH_3Cl, CF_3Cl, CF_2Cl_2, $CFCl_3$ and C_2H_5Cl

A similar approach was employed for the kinetic investigation of Cs(6 $^2S_{1/2}$) + CH_3Cl, CF_3Cl, CF_2Cl_2, $CFCl_3$ and C_2H_5Cl as that described above for the study of the rate data for atomic caesium with nitrous oxide using the analysis based on equations (1), (3) and (4). LIF decay profiles for Cs(6 $^2S_{1/2}$), similar to those shown in Fig. 5 were recorded within the limited temperature range 780–830 K in the presence of these chloride reactants at fixed fractional compositions and excess He buffer gas. Plots of $k'p_T$ vs. p_T^2 were constructed. These are shown in Figs. 7–9, the slopes of which, coupled with the values of f (= [RCl]/([RCl] + [He])), yield the absolute second-order rate constants for reaction at a given temperature (Eq. (4)). The intercepts of the plots of $k'p_T$ vs. p_T^2 were found to yield values of β (Eq. (4)) which are similar to those obtained from slopes of plots of the type given in Fig. 4 and that these are relatively small in relation to the magnitude of the ordinate (Figs. 7–9), indicating the dominance of chemical reaction in the removal of Cs(6 $^2S_{1/2}$) by these chlorides.

The rate data for the removal of Cs by CH_3Cl does not permit characterization of the Arrhenius parameters over the

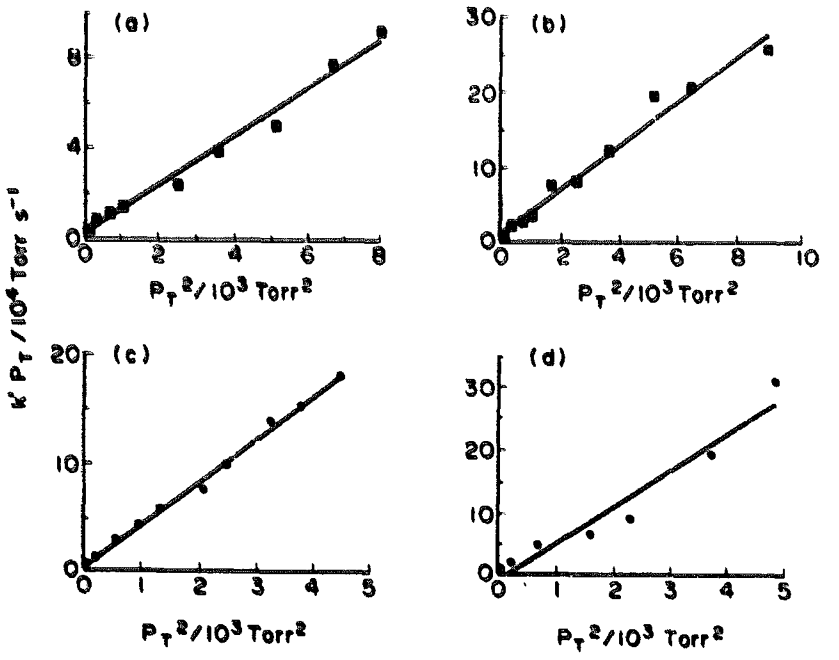

Fig. 8. Examples of the variation in the first-order decay coefficient k' for the decay of Cs(6 $^2S_{1/2}$) obtained by LIF at λ = 455.5 nm (Cs(7 $^2P_{3/2}$–6 $^2S_{1/2}$)) following the pulsed irradiation of CsCl vapour in the presence of different total pressures p_T of CF_3Cl and CF_2Cl_2 with helium buffer gas i.e. $k'p_T$ vs. p_T^2 at different temperatures (f = [RCl]/([He] + [RCl])): (a) CF_3Cl, T = 800 K, $f = 3.9 \times 10^{-5}$; (b) CF_3Cl, T = 830 K, $f = 8.4 \times 10^{-5}$; (c) CF_2Cl_2, T = 780 K, $f = 2.8 \times 10^{-5}$; (d) CF_2Cl_2, T = 830 K, $f = 3.1 \times 10^{-5}$.

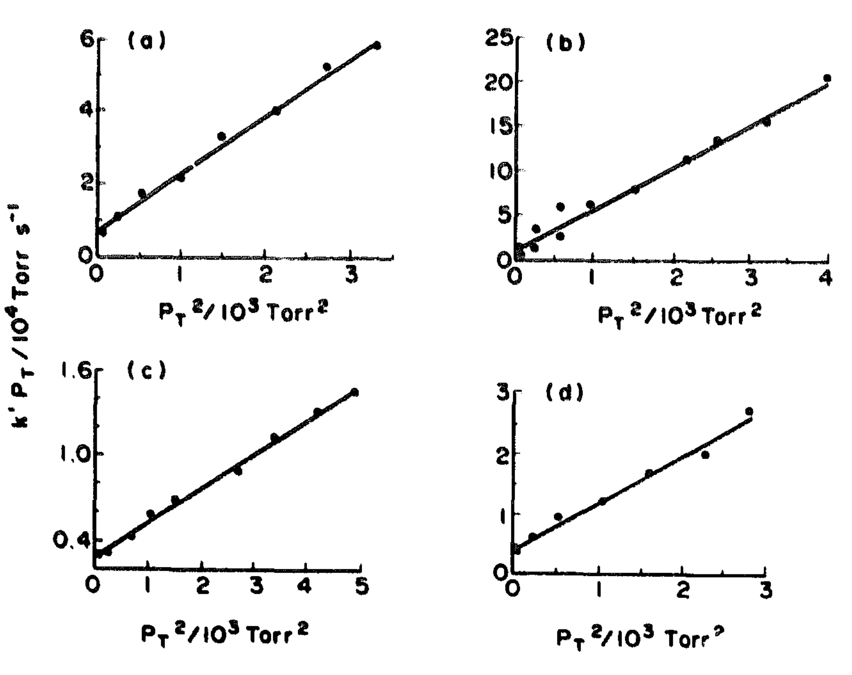

Fig. 9. Examples of the variation in the first-order decay coefficient k' for the decay of Cs(6 $^2S_{1/2}$) obtained by LIF at λ = 455.5 nm (Cs(7 $^2P_{3/2}$–6 $^2S_{1/2}$)) following the pulsed irradiation of CsCl vapour in the presence of different total pressures p_T of $CFCl_3$ and C_2H_5Cl with helium buffer gas i.e. $k'p_T$ vs. p_T^2 at different temperatures (f = [RCl]/([He] + [RCl])): (a) $CFCl_3$, T = 780 K, $f = 1.5 \times 10^{-5}$; (b) $CFCl_3$, T = 830 K, $f = 3.4 \times 10^{-5}$; (c) C_2H_5Cl, T = 780 K, $f = 3.2 \times 10^{-5}$; (d) C_2H_5Cl, T = 830 K, $f = 2.9 \times 10^{-5}$.

narrow temperature range employed. The average result for $T = 830$ K yields $k_R(Cs + CH_3Cl, T = 830\ K) = (5.4 \pm 0.2) \times 10^{-12}$ cm^3 molecule^{-1} s^{-1} which can be compared with analogous data determined by time-resolved atomic resonance absorption spectroscopy at $\lambda = 455.5$ nm ($Cs(7\ ^2P_{1/2}) \leftarrow Cs(6\ ^2S_{1/2})$) of $k_R(Cs + CH_3Cl, T = 830\ K) = (6.9 \pm 0.7) \times 10^{-12}$ cm^3 molecule^{-1} s^{-1} [16] which is sensible agreement by the two methods. The analogous comparison of $k_R(Cs + CF_3Cl, T = 830\ K) = (3.0 \pm 0.2) \times 10^{-11}$ cm^3 molecule^{-1} s^{-1} determined in this investigation by LIF with that obtained by time-resolved atomic resonance absorption spectroscopy of $k_R(Cs + CF_3Cl, T = 830\ K) = (2.7 \pm 0.2) \times 10^{-11}$ cm^3 molecule^{-1} s^{-1} [16] again indicates agreement between the two methods. The present result for $k_R(Cs + CF_2Cl_2, T = 830\ K) = (1.5 \pm 0.5) \times 10^{-11}$ cm^3 molecule^{-1} s^{-1} obtained by LIF is marginally larger than that obtained by atomic resonance absorption spectroscopy of $k_R(Cs + CF_2Cl_2, T = 830\ K) = (9.0 \pm 1.5) \times 10^{-12}$ cm^3 molecule^{-1} s^{-1} [16] but still indicating sensible agreement between the two methods. Similarly, the result for $k_R(Cs + C_2H_5Cl, T = 830\ K) = (1.5 \pm 0.5) \times 10^{-11}$ cm^3 molecule^{-1} s^{-1} obtained here by LIF is marginally larger than that derived from atomic resonance absorption spectroscopy of $k_R(Cs + C_2H_5Cl, T = 830\ K) = (9.5 \pm 0.8) \times 10^{-12}$ cm^3 molecule^{-1} s^{-1} [16] taken at the same wavelength. The result for $k_R(Cs + CFCl_3, T = 830\ K) = (1.2 \pm 0.1) \times 10^{-10}$ cm^3 molecule^{-1} s^{-1} obtained here by LIF, however, is significantly larger than that reported from atomic resonance absorption spectroscopy where $k_R(Cs + CFCl_3, T = 830\ K) = (4.8 \pm 0.8) \times 10^{-12}$ cm^3 molecule^{-1} s^{-1} [16]. We may only conclude significant thermal decomposition of $CFCl_3$ under the conditions of the static reactor employed [16].

The thermochemistry for these Cl-atom abstraction reactions by atomic caesium is highly exothermic in all cases ($D(CsCl(X\ ^1\Sigma^+)) = 444 \pm 13$ kJ mol^{-1} [33]; $D(CF_3$–$Cl) = 360.2 \pm 3.3$ kJ mol^{-1} [34]; $D(CF_2Cl$–$Cl)$, 346.0 ± 13.4 kJ mol^{-1} [34]; $D(CFCl_2$–$Cl)$, 305 ± 8 kJ mol^{-1} [34]; $D(CH_3$–$Cl)$, 349 kJ mol^{-1}; $D(C_2H_5Cl)$, 341 kJ mol^{-1} [35–38] ($\Delta H \approx -75$ to -160 kJ mol^{-1}). As indicated in the atomic resonance absorption measurements [16], it is difficult to estimate the effects of the photodissociation of the chlorinated precursors where the kinetic effects would be larger for the multichlorinated reactants. Both the present LIF method and the absorption technique used hitherto [16] employ broad-band photolysis. The reactant concentrations employed in both investigations are low as seen from the values of f employed here and earlier [16] and, given that the rate data for Cs indicate reactivities proceeding with efficiencies relatively close to those of the collision numbers, the kinetic effects of small yields of photodissociation products from the precursors should be small. Overall, the rate data for $Cs(6\ ^2S_{1/2})$ with these chlorides proceed rapidly, clearly involving only small energy barriers for Cl abstraction. Apart from the reaction between Cs and $CFCl_3$, there is reasonable agreement between the kinetic results for the chlorides obtained by the present LIF measurements and those from atomic absorption spectroscopy [16]. Whilst the present result for $k_R(Cs + N_2O)$ is significantly larger than that obtained by the absorption spectroscopic method [13], it is in good agreement with that reported from LIF measurements given by Plane [3], supporting the LIF technique described here for determining the present rate data for $Cs(6\ ^2S_{1/2})$ at an elevated temperature.

Acknowledgement

The authors gratefully acknowledge the financial support provided by the Spanish Direccion General de Investigacion Cientifica y Tecnica (Project PB91-0309).

References

[1] D. Husain, *J. Chem. Soc., Faraday Trans. II, 85* (1989) 85.
[2] J.M.C. Plane, *Int. Rev. Phys. Chem., 10* (1991) 55.
[3] J.M.C. Plane, A comparison between the oxidation reactions of alkali and alkaline earth atoms, in A. Fontijn (ed.), *Gas Phase Metal Reactions*, North-Holland, Amsterdam, 1992, p. 29.
[4] D.R. Lide and H.P.R. Frederikse (eds.), *CRC Handbook of Chemistry and Physics*, CRC Press, Boca Raton, FL, 75th edn., 1994–1995, p. 10-206.
[5] A.F. Ashton and A.N. Hayhurst, *J. Chem. Soc., Faraday Trans. I, 69* (1973) 652.
[6] W.E. Kaskan, *Proc. 10th Int. Symp. on Combustion*, Academic Press, New York, 1965, p. 141.
[7] R. Carabetta and W.E. Kaskan, *J. Phys. Chem., 72* (1968) 2483.
[8] T.H. Bull and P.B. Moon, *Discuss Faraday Soc., 17* (1954) 54.
[9] D.C. Brodhead, P. Davidovits and S.A. Edelstein, *J. Chem. Phys., 51* (1989) 3601.
[10] S.A. Edelstein and P. Davidovits, *J. Chem. Phys., 55* (1971) 5164.
[11] J. Maya and P. Davidovits, *J. Chem. Phys., 59* (1973) 3143.
[12] J. Maya and P. Davidovits, *J. Chem. Phys., 61* (1974) 1082.
[13] D. Husain and Bing Ji, *J. Photochem. Photobiol. A: Chem., 53* (1990) 1.
[14] D. Husain and Bing Ji, *J. Photochem. Photobiol. A: Chem., 53* (1990) 169.
[15] R.S. Clay and D. Husain, *J. Chem. Res.*, (1990) (S) 384, (M) 2944.
[16] R.S. Clay and D. Husain, *J. Photochem. Photobiol. A: Chem., 56* (1991) 1.
[17] D. Husain, J.M.C. Plane and Chen Cong Xiang, *J. Chem. Soc., Faraday Trans. II, 81* (1985) 769.
[18] D. Husain, J.M.C. Plane and Chen Cong Xiang, *J. Chem. Soc., Faraday Trans. II, 81* (1985).
[19] L.W. Grossman, G.S. Hurst, S.D. Kramer, M.G. Payne and J.P. Young, *Chem. Phys. Lett., 50* (1977) 207.
[20] G.S. Hurst, M.H. Nayfeh and J.P. Young, *Appl. Phys. Lett., 30* (1977) 229.
[21] G.S. Hurst, M.H. Nayfeh and J.P. Young, *Phys. Rev. Lett., 15* (1977) 2283.
[22] J.M.C. Plane, *J. Phys. Chem., 91* (1987) 6552.
[23] J.M.C. Plane and B. Rajasekhar, *J. Phys. Chem., 93* (1989) 3135.
[24] J.M.C. Plane, B. Rajeskehar and L. Bartolloti, *J. Phys. Chem., 94* (1990) 4161.

[25] C.E. Moore (ed.), *Atomic Energy Levels, Natl. Bur. Stand. Circ., 467,* Vol. III, 1958, p. 124 (US Government Printing Office, Washington, DC).

[26] C.H. Corliss and W.R. Bozman, *Experimental Transition Probabilities of Spectral Lines of Seventy Elements, US Monograph 53,* US Government Printing Office, Washington, DC, 1962, p. 79.

[27] G.E. Cogin and C.E. Kimball, *J. Chem. Phys., 16* (1948) 1035.

[28] P. Davidovits and D.C. Brodhead, *J. Chem. Phys., 46* (1967) 2698.

[29] D.R. Lide and H.P.R. Frederikse (eds.), *CRC Handbook of Physics and Chemistry,* CRC Press, Boca Raton, FL, 75th edn., 1994–1995, p. 10-137.

[30] D. Husain and R.J. Donovan, *Adv. Photochem., 8* (1971) 1.

[31] A.C.G. Mitchell and M.W. Zemansky, *Resonance Radiation and Excited Atoms,* Cambridge University Press, London, 1961.

[32] M.W. Zemansky, *Phys. Rev., 34* (1929) 313.

[33] A.A. Radzig and B.M. Smirnov, *Reference Data on Atoms, Molecules and Ions,* Springer, Berlin, 1985, p. 378.

[34] D.R. Lide and H.P.R. Frederikse (eds.), *CRC Handbook of Chemistry and Physics,* CRC Press, Boca Raton, FL, 75th edn., 1994–1995, p. 9-51.

[35] R.C. Weast, M.J. Astle and W.H. Beyer (eds.), *CRC Handbook of Physics and Chemistry,* CRC Press, Boca Raton, FL, 69th edn., 1988–1989.

[36] S.W. Benson, *Thermochemical Kinetics,* Wiley–Interscience, New York, 1976.

[37] V.I. Vedeneyev, L.V. Gurvich, V.N. Kondratiev, V.A. Medvedev and Ye.L. Frankevitch, *Bond Energies, Ionisation Potentials and Electron Affinities,* Nauka, Moscow, 1974.

[38] J.D. Cox and G. Pilcher, *Thermochemistry of Organic and Organometallic Compounds,* Academic Press, London, 1970.